

## ADVANCES IN THE UNDERSTANDING OF THE STRUCTURE-FUNCTION RELATIONSHIP IN Cu,Zn SUPEROXIDE DISMUTASE

L. BANCÌ\*, I. BERTINI\*, D.E. CABELLI‡, R.A. HALLEWELL‡,  
C. LUCHINAT† and M.S. VIEZZOLI\*

\**Department of Chemistry, University of Florence, Florence, Italy;* ‡*Brookhaven National Laboratory, Upton, New York 11973, U.S.A.;* §*Chiron Corporation, Emeryville, CA 94608, U.S.A.;* ¶*Institute of Agricultural Chemistry, University of Bologna, Bologna, Italy*

The structure-function relationship in Cu,Zn superoxide dismutase has been partially elucidated by the combined use of many spectroscopic techniques (electronic spectroscopy, circular dichroism, EPR and NMR) and site-directed mutagenesis techniques. The comparison of the spectroscopic and catalytic properties of various mutants, in which some active site residues have been substituted through site-directed mutagenesis, allowed us to establish that the activity is in general more sensitive to electrostatic effects rather than to steric effects or changes in the copper hydration or coordination geometry.

**KEY WORDS:** Superoxide dismutase, metallo protein, copper, zinc, mutants, site-directed mutagenesis, electrostatic effects.

### INTRODUCTION

The aim of the present paper is to survey the most recent studies carried out in our laboratories on Cu,Zn superoxide dismutase (SOD hereafter). The use of many spectroscopic techniques (electronic spectroscopy, circular dichroism, EPR and NMR) has allowed us to partially elucidate the structure-function relationship in this enzyme. The environment of the metals, in particular the copper site, where the catalytic reaction occurs, has been studied. Our research has addressed both the characterization of the coordination geometry around the metal ions in the native protein, and the establishment of the role of the amino acid residues in the catalytic cavity. With this purpose, some residues of the active site have been substituted through site directed mutagenesis, and the spectroscopic and functional properties of the new derivatives have been compared with those of the wild type enzyme.

### THE COORDINATION PROPERTIES OF THE COPPER CHROMOPHORE

At the present time, several spectroscopic information concerning the copper chromophore in the native enzyme are available.<sup>1-3</sup> X-ray diffraction studies on the bovine enzyme<sup>4</sup> have shown that four histidines are coordinated to the copper(II) ion. One

Prof. Ivano Bertini, Department of Chemistry, University of Florence, Via G. Capponi 7, 50121 Florence, Italy.

water molecule is bound to copper, at a Cu-O distance of 0.28 nm.<sup>5</sup> One of the histidines coordinated to copper(II) is a bridging ligand to the zinc(II) ion. The coordination around zinc(II) is completed by two more histidines and one aspartate residue. A scheme of the metal sites is reported in Figure 1. The human and the yeast enzyme show very high homology with the bovine enzyme, as all the residues in the active cavity are conserved.<sup>6-8</sup>

The electronic spectrum of the enzyme shows a broad band centered around 14000 cm<sup>-1</sup> and other ill-resolved absorptions above 20000 cm<sup>-1</sup>.<sup>9</sup> The CD spectrum shows a negative band at about 13000 cm<sup>-1</sup>, and two positive bands at 16-17000 cm<sup>-1</sup> and around 22-25000 cm<sup>-1</sup>. This last absorption is weaker than the others. Two strong bands are observed around 30000 cm<sup>-1</sup>. The two lowest energy absorptions have been assigned to d-d transitions, while the shoulder at 22-25000 cm<sup>-1</sup> has been attributed to either a d-d transition or a ligand-to-metal charge transfer (LMCT) arising from the bridging imidazolato residue. The UV bands have been assigned as LMCT.<sup>9,10</sup>

The EPR spectra are characterized by a rhombic distortion and by a resolved hyperfine structure in the  $g_{\parallel}$  region.<sup>11</sup> The  $A_{\parallel}$  value has been estimated  $142 \times 10^{-4}$  cm<sup>-1</sup> for solutions of Cu,Zn human SOD expressed in yeast, at room temperature.<sup>11c</sup>

Water <sup>1</sup>H Nuclear Magnetic Relaxation Dispersion (NMRD) measurements performed on solutions of Cu,Zn SOD indicate the presence of exchangeable protons in the active cavity.<sup>12,13</sup> If they arise from a coordinated water molecule the analysis of the data yields an average Cu-H distance of 0.33 nm (Cu-O = 0.24 nm).<sup>13</sup>

The spectroscopic data can be interpreted, in agreement with the X-ray structure,

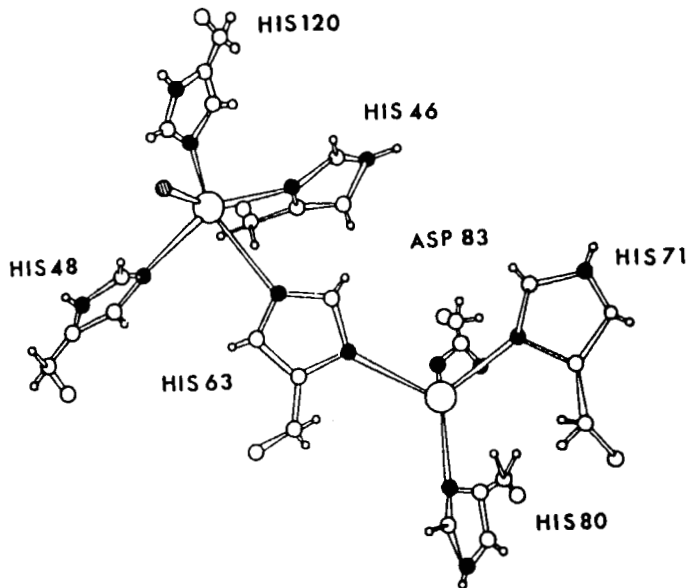


FIGURE 1 Schematic drawing of the metal sites of SOD. The numbering of the residues is that of the human enzyme.

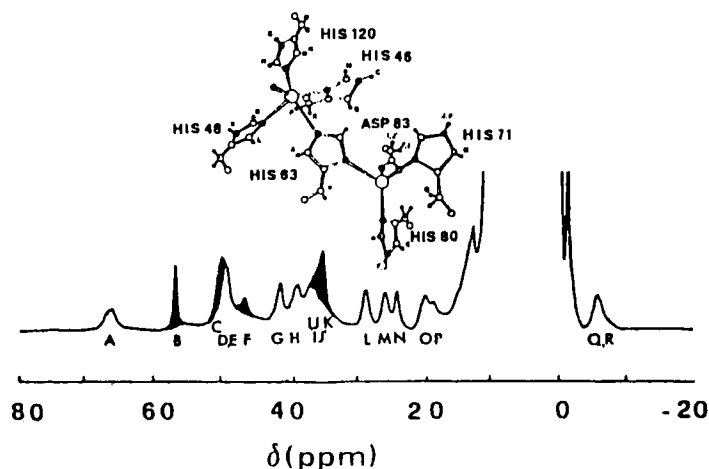


FIGURE 2 200 MHz  $^1\text{H}$  NMR spectrum of  $\text{Cu}_2\text{Co}_2$  wild type SOD. The spectra are recorded at 300 K. The samples are in 50 mM Hepes buffer, pH 7.5. The filled signals disappear in  $\text{D}_2\text{O}$ . The letters indicate the proposed assignment.

in terms of a distorted square pyramidal copper chromophore with a water molecule weakly bound in the apical position.

The native metal ions can be easily substituted by several other metal ions.<sup>2</sup> Among the many derivatives that can be obtained, the derivative in which Zn(II) has been substituted by Co(II),  $\text{Cu}_2\text{Co}_2\text{SOD}$ , is very suitable for  $^1\text{H}$  NMR characterization of the active site. Indeed, the isotropic shift induced by the presence of high spin Co(II), allows us to observe well resolved and sharp  $^1\text{H}$  NMR signals of protons of residues bound to the metal ion.<sup>14</sup> Furthermore, magnetic coupling through the histidinato bridge between copper(II) and cobalt(II) causes a decrease in the electronic relaxation time of copper and also permits the observation of sharp lines of the protons in the environment of the copper ion.<sup>14,15</sup> The  $^1\text{H}$  NMR spectrum of the  $\text{Cu}_2\text{Co}_2$ -derivative, reported in Figure 2, has been completely assigned, and its features correlated with structural properties.<sup>16-18</sup> We note that the shifts of protons belonging to His-48 ring (signals K, L, and O) are the smallest among the signals of the other histidines coordinated to copper. This behavior can be reasonably explained on the basis of a slightly longer  $\text{Cu}-\text{N}_{(\text{His-48})}$  distance. His-48 seems to be more weakly bound to Cu(II) than the other three histidines.

The electronic and EPR parameters of SOD have been interpreted by us through the application of the Angular Overlap Model (AOM).<sup>19-21</sup> Extensive calculations have been performed in order to find AO parameters that can reproduce the experimental data (CD and EPR spectra) of the wild type as well as of the mutants and of the anions adducts.<sup>22</sup> We have been able to reproduce the spectra of several mutants and to relate them to geometrical changes in these derivatives. In particular, it has been possible to reproduce the experimental electronic transitions and the EPR parameters by assigning equal  $e_\sigma$  values ( $8 \times 10^3 \text{ cm}^{-1}$ ) to three out of the four histidines coordinated to copper(II), and half of this value to His-48; a decrease in the strength of the Cu-N bond for this histidine has been decided following the indications given by the  $^1\text{H}$  NMR spectrum of  $\text{Cu}_2\text{Co}_2\text{SOD}$ . The geometric parameters of

the X-ray structure<sup>4</sup> were used throughout. A value of  $e_p = 0$  is assigned to the oxygen of the water molecule. The assignment of  $e_p$  values higher than 0 for the Cu–O bond, produces changes in the transition energies and in the EPR parameters that are contrary to the observation. Therefore, the presence of water seems to be irrelevant in the computation of the transition energies,<sup>22</sup> in agreement with the very long Cu–O distance found from X-ray<sup>4</sup> and NMRD<sup>12</sup> data.

### THE INFLUENCE OF NON COORDINATED RESIDUES ON THE STRUCTURAL ARRANGEMENT OF THE ACTIVE SITE

In order to investigate the relationship between structure and function, some aminoacids present in the catalytic site and not directly coordinated to the metal ions have been substituted through site-directed mutagenesis.<sup>23</sup> These modifications have been performed on the human isoenzyme expressed in either *E. coli* or yeast cells.<sup>24,25</sup> Thr-137 and Arg-143, the residues at the entrance of the catalytic pocket (Figure 3), have been substituted with Ser, Ala, Ile,<sup>26,27</sup> and Lys, Ile, Glu<sup>28,29</sup> respectively. Asp-124, that forms a long range bridge between copper and zinc connecting His-46 (one of the ligands of Cu) to His-71 (one of the ligands of Zn) through hydrogen bonding (Figure 3), has been substituted with Asn and Gly. Glu-133 is a negative residue just at the entrance of the cavity (Figure 3) and might interact either with the coordinated water<sup>4</sup> or with the OH of Thr-137 through hydrogen bonding;<sup>5</sup> it has been substituted by Gln. Next to each of these two negative residues, Asp-124 and Glu-133, there is an additional negative group, namely Asp-125 and Glu-132, respectively. We have prepared also mutagenized derivatives in which both Asp-124 and Asp-125, or both Glu-132 and Glu-133, are substituted by Asn and Gln, respectively.

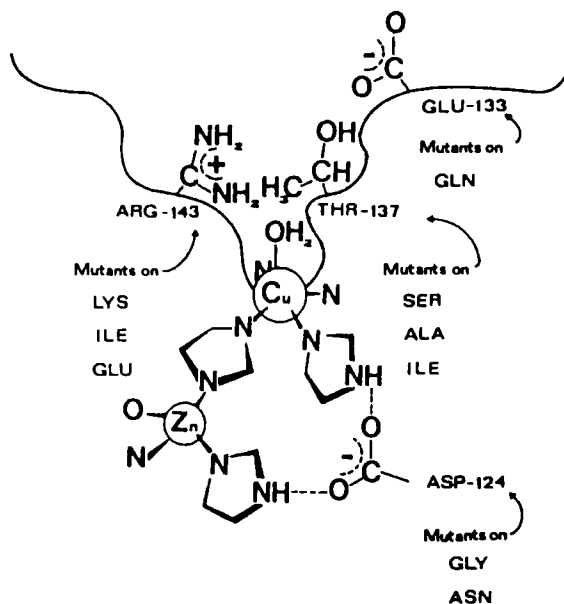


FIGURE 3 Schematic drawing of the active cavity of SOD and of the mutations obtained on some residues.

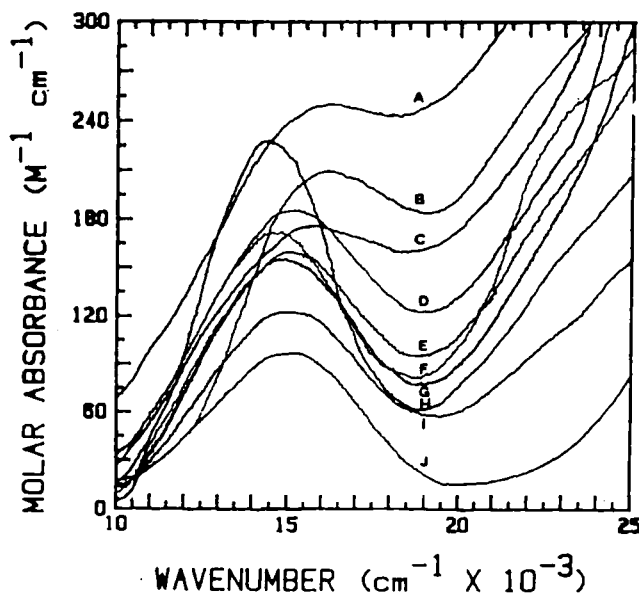


FIGURE 4 Visible electronic spectra of: A) Asn-124Asn-125; B) Ile-137; C) Asn-124; D) Gln-133; E) Ala-137; F) Ser-137; G) Gln-132; H) wild type SOD; I) Gln-132Gln-133; J) Gly-124.

All the mutants contain approximately two equivalents of copper and zinc per dimer, except the mutants on the 124 position that show a dramatically lower content of zinc (15% for Asn-124, 5% for Gly-124 and <1% for Asn-124Asn-125).

The electronic spectra for some of the mutants on the 137, 124/125 and 132/133 positions are reported in Figure 4 together with that of the wild type enzyme. Ala-137, Ile-137 and Asn-124Asn-125 mutants all show a shift, albeit to different extents, of the d-d transitions toward higher energies with respect to the wild type.<sup>22,26</sup>

In Table I the room temperature EPR parameters of solutions of these mutants are reported. The  $A_{\parallel}$  values range between 137 and  $162 \times 10^{-4} \text{ cm}^{-1}$ , and their increase roughly parallels an axialization of the spectrum. Indeed, it appears that the largest  $A_{\parallel}$  values are provided by the Ile-137, Gly-124, Asn-124, Asn-124Asn-125, that show an axial EPR spectrum (see Figure 5).

Water NMRD measurements are a powerful method for determining the presence of water molecules interacting with a paramagnetic metal ion.<sup>30,31</sup> Among the 137-mutants,<sup>26</sup> the data show that there is a trend in decreasing the amount of water interacting with the copper(II) ion. The amount of water follows the order: Ser-137 > Thr-137  $\cong$  Ala-137 > Ile-137. This trend could be related to the bulkiness and hydrophobicity of the residue. In the case of Ile-137 the paramagnetic effect detected through  $^1\text{H}$ NMRD on the water protons is so low that it is reasonable to conclude that no first sphere water interacts with the copper ion.

The  $^1\text{H}$ NMR spectra of the  $\text{Cu}_2\text{CO}_2$ -derivatives of the 137-mutants show a close similarity with those of the wild type (Figure 6).<sup>26</sup> However, for Ala-137 and, to a greater extent, for Ile-137 it is possible to observe a larger downfield shift (see Table II) for the signals belonging to His-48 (signals K, L and O). This behavior can be attributed to a stronger Cu-N bond of His-48. Therefore it seems that, parallel to the

TABLE I  
 EPR Parameters of some SOD Derivatives

	$A_{\parallel}$ ( $\text{cm}^{-1} \times 10^4$ )	$g_{\parallel}$	$g_{\perp}^d$	shape
WT (yeast)	142	2.28	(2.09)	rhombic <sup>b</sup>
WT ( <i>E. coli</i> )	138	2.26	(2.09)	rhombic <sup>b</sup>
Ser 137	140	2.26	(2.07)	rhombic <sup>c</sup>
Ala 137	139	2.26	(2.07)	rhombic <sup>c</sup>
Ile 137	162	2.25	2.04	axial <sup>b</sup>
Lys 143	150	2.25	2.07	axial <sup>b</sup>
Ile 143	137	2.26	(2.08)	rhombic <sup>b</sup>
Glu 143	148	2.28	2.09	axial <sup>b</sup>
Gln 132	140	2.26	(2.07)	rhombic <sup>d</sup>
Gln 133	142	2.26	(2.07)	rhombic <sup>d</sup>
Gln 132 Gln 133	136	2.26	(2.07)	rhombic <sup>d</sup>
Gly 124	155	2.27	2.06	axial <sup>d</sup>
Asn 124	155	2.26	(2.06)	rhombic <sup>d</sup>
Asn 124 Asn 125	154	2.26	2.06	axial <sup>d</sup>
$\text{Cu}_2\text{E}_2\text{WT}$	154	2.27	2.05	axial <sup>d</sup>

<sup>a</sup>the number in parenthesis for the  $g_{\perp}$  region of the EPR spectrum in rhombic systems, represents the reading at zero intensity on the left side of  $g_{\parallel} + g_{\perp}$  feature in the first derivative spectra; <sup>b</sup>reference 11; <sup>c</sup>reference 26; <sup>d</sup>reference 22.

decrease of the Cu–OH<sub>2</sub> interaction, His-48 is more strongly bound and the chromophore tends to reach an almost regular square planar geometry with the copper ion in the plane defined by the four histidine nitrogens. For the mutants on position 143 and 132/133 much smaller perturbations on the <sup>1</sup>H NMR spectrum of the active site are induced by the residue substitution.

The CD spectra of all the mutants studied up to now have been recorded and analyzed in terms of gaussian functions to estimate the transition energies more accurately.<sup>22</sup> In Table III, the results of this analysis are shown. As far as the d-d transitions are concerned, the lowest energy band is always in the range 13000–13700  $\text{cm}^{-1}$  with the exception of Ile-137, Glu-143 and Lys-143 (at about 14000  $\text{cm}^{-1}$ ). Another band is centered around 16000  $\text{cm}^{-1}$  and it is of low intensity in the derivatives that are zinc deficient, such as the 124-mutants. In the case of Asn-124, it can be resolved in two bands separated by less than 1000  $\text{cm}^{-1}$ . Also in the zinc-free derivative,  $\text{Cu}_2\text{E}_2\text{SOD}$ , ( $E = \text{empty}$ ), a third band has been reported at about 18000  $\text{cm}^{-1}$ .<sup>9</sup> The EPR spectra of the 124 mutants show an increase of the  $A_{\parallel}$  value and a decrease in rhombicity, in agreement with a structure close to that of  $\text{Cu}_2\text{E}_2\text{SOD}$ <sup>12</sup> (see Table I). The EPR spectra are not pH dependent up to pH 9.2. This indicates that here migration of copper does not occur, in contrast with  $\text{Cu}_2\text{E}_2\text{SOD}$ , in which copper migrates into the empty zinc site above pH 7. Under drastic conditions (extensive dialysis against 0.5 M metal salt solution), it is possible to bind either zinc(II) or cobalt(II) to the zinc site, obtaining copper-zinc and copper-cobalt derivatives. The copper-zinc derivative of the Asn-124 mutant shows an  $A_{\parallel}$  value close to that of the wild type. Therefore, the removal of the long range bridge between His-46 and His-71 in the 124 mutants seems to induce some structural variations in the zinc site making the binding process difficult, possibly from a kinetic point of view. However, once a metal is bound into the zinc site, the active site essentially restores the native conformation.

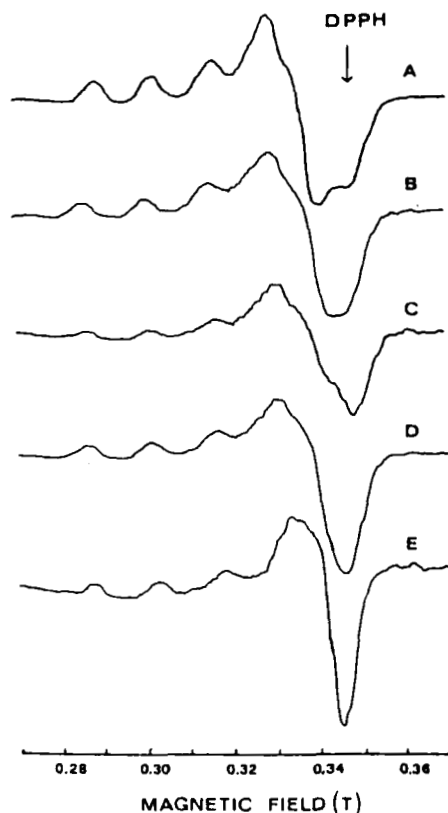


FIGURE 5 Room temperature 9.81 GHz EPR spectra of A) wild type SOD; B) Gly-124; C) Asn-124; D) Asn-124Asn-125; E) Ile-137. Conditions were the same as in Figure 2.

We have applied the AOM analysis to the mutants to reproduce the changes observed in the electronic transitions and in the EPR parameters with respect to the wild type enzyme.<sup>22</sup> Starting with the same set of parameters chosen for the wild type and simultaneously i) changing the polar angles  $\theta$  and  $\phi$  of His-48 in the direction of making a more square planar geometry and ii) increasing the  $\epsilon_r$  of His-48 (Figure 7 from left to right) it has been possible to obtain a qualitative agreement with the experimental transition energies and the EPR parameters observed in the mutants. Therefore, it seems possible to reproduce the trends in the electronic transitions and EPR parameters for all the mutants, just by relatively minor adjustments of the binding mode of His-48.

We are presently trying to rationalize the experimental data of the adducts of SOD with some anions ( $\text{N}_3^-$ ,  $\text{CN}^-$ ,  $\text{CNO}^-$ ,  $\text{NCS}^-$ , etc.) by using the same model.

A careful evaluation of the activity of these mutants, performed through pulse radiolysis,<sup>27,33</sup> is essential to have information about the role of the residues in the mechanism of the reaction. It has been previously observed that the substitution of Arg 143 with any other residue, positive (like Lys), or neutral (like Ile), or negatively charged (like Glu) leads to a decrease in activity in the pH range 5–12. At neutral pH the activity is 49% for Lys, 11% for Ile and < 1% for Glu with respect to the value

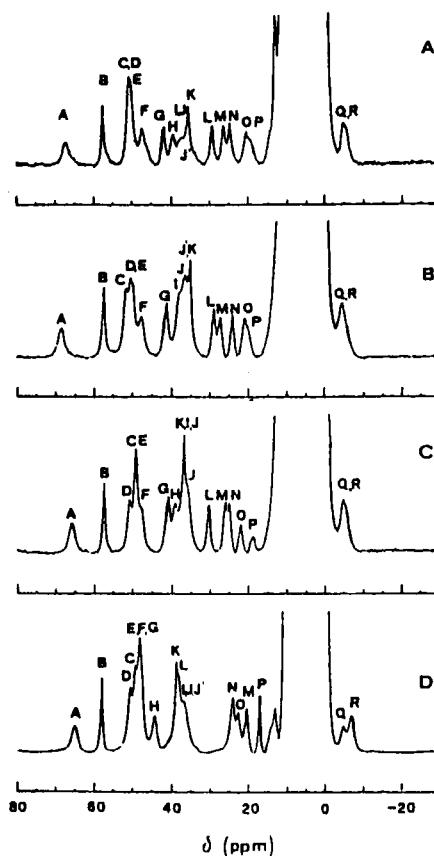


FIGURE 6 200 MHz  $^1\text{H}$  NMR spectra in  $\text{H}_2\text{O}$  of A)  $\text{Cu}_2\text{Co}_2$ -wild type SOD; B)  $\text{Cu}_2\text{Co}_2$ Ser-137; C)  $\text{Cu}_2\text{Co}_2$ Ala-137; D)  $\text{Cu}_2\text{Co}_2$ Ile-137. Conditions were the same as in Figure 2.

of the wild type.<sup>29,34,35</sup> As substitution of Lys for Arg leads to the smallest reduction in activity, the positive charge of Arg-143 appears to be very important in the catalytic reaction, possibly for the molecular recognition of the substrate.

The activity profiles as a function of pH for the 137 mutants, together with that of the wild type, are reported in Figure 8. All the profiles of the mutants are similar to that of the wild type, showing a slight decrease in activity around pH 7 and then a large decrease at alkaline pH. The activity is not substantially varied in these mutants, although they show a reduced amount of water at the active site. These results suggest that the redox reaction between copper and superoxide is not mediated by water, or at least by the water in the active site cavity.

Substitution at position 132 does not affect the activity profile (Figure 9) indicating that this residue does not seem to have an important role in the reaction. The activity of the Gln-133 and Gln-132Gln-133 mutants has almost the same value as that of the wild type at low pH, while at physiological pH the activity drops to 33% and 48% of the wild type, for Gln-133 and Gln-132Gln-133, respectively. This behavior is not easily explained, as the removal of a negative charge might be expected to increase the



TABLE II

Chemical Shifts (in ppm) of the  $^1\text{H}$  NMR Signals of the Wild Type and of the 137 Mutants of  $\text{Cu}_2\text{Co}_2\text{SOD}$  Derivatives at 200 MHz, 300 K.

Signal	WT	Ser-137	Ala-137	Ile-137	Assignment
A	66.3	67.8	65.4	64.7	His-63 H $\delta$ 2
B	56.9	56.8	56.9	57.6	His-120 H $\delta$ 1
C	50.0	50.9	48.6	48.8	His-46 H $\epsilon$ 2
D	49.6	49.8	50.2	50.2	His-80 H $\delta$ 2 (His-71 H $\delta$ 2)
E	49.2	49.8	48.6	47.7	His-71 H $\delta$ 2 (His-80 H $\delta$ 2)
F	46.8	47.0	47.2	47.7	His-80 H $\epsilon$ 2 (His-71 H $\epsilon$ 2)
G	41.4	40.8	40.5	47.7	His-46 H $\delta$ 2
H	39.1	37.9	38.7	43.8	His-120 H $\epsilon$ 1
I	36.9	36.0	36.3	36.5	Asp-83 H $\beta$ 1 (Asp-83 H $\beta$ 2)
J'	36.0	36.0	36.3	36.5	Asp-83 H $\beta$ 2 (Asp-83 H $\beta$ 1)
J	35.6	34.5	35.5	36.5	His-71 H $\epsilon$ 2 (His-80 H $\epsilon$ 2)
K	35.0	34.5	36.3	38.5	His-48 H $\delta$ 1
L	28.8	28.3	29.9	37.9	His-48 H $\delta$ 2
M	25.8	26.7	25.5	20.2	His-46 H $\epsilon$ 1
N	24.1	23.5	24.5	23.8	His-120 H $\delta$ 2
O	19.8	20.3	21.4	22.4	His-48 H $\epsilon$ 1
P	18.9	19.4	18.5	16.7	His-46 H $\beta$ 1
Q	-5.7	-4.8	-5.3	-5.3	His-46 H $\beta$ 2 (-)
R	-5.7	-4.8	-5.3	-7.3	- (His-46 H $\beta$ 2)

affinity for the superoxide anion. Current experiments should aid in elucidating this point.

### CONCLUDING REMARKS

In conclusion, site directed mutagenesis, in combination with many spectroscopic techniques (EPR, CD,  $^1\text{H}$ NMR, Water  $^1\text{H}$ NMRD) and pulse radiolysis, is a very

TABLE III  
Energies of the Electronic Transitions from CD Measurements (in  $\text{cm}^{-1} \times 10^{-3}$ )<sup>a</sup>

WT (yeast)	13.3(-)	16.7(+)		22.4(+)	29.6(+)	33.0(+)
yeast	13.3(-)	15.9(+)		22.0(+)	28.7(+)	38.4(+)
Ser 137	13.0(-)	16.7(+)		23.2(+)	29.9(+)	32.4(+)
Ala 137	13.7(-)	15.6(+)		22.0(+)	30.0(+)	32.0(+)
Ile 137	14.3(-)	17.5(+)		25.2(+)	28.5(+)	32.4(+)
Lys 143	14.0(-)	16.8(+)		25.0(+)	29.4(+)	
Ile 143	13.7(-)	16.5(+)		25.3(+)	29.4(+)	
Glu 143	14.3(-)	16.9(+)		25.3(+)	30.3(+)	33.9(+)
Gln 132	13.5(-)	16.5(+)		24.6(+)	29.3(+)	33.1(+)
Gln 133	13.6(-)	16.4(+)		21.5(+)	29.4(+)	32.1(+)
Gln 132 Gln 133	13.6(-)	16.2(+)		25.9(+)	29.4(+)	32.0(+)
Asn 124	13.3(-)	16.5(+)	17.4(+)	22.8(+)	30.7(+)	32.8(+)
Gly 124	13.3(-)	16.5(+)		25.6(-)	31.0(+)	
Asn 124 Asn 125	13.1(-)	17.1(+)		26.3(-)		31.4(+)
$\text{Cu}_2\text{E}_2\text{WT}^b$	12.5(-)	16.2(+)	18.0(+)		31.0(+)	

<sup>a</sup>obtained through a computer simulation of the spectra using Gaussian line-shapes. The signs of the bands are reported in parenthesis. The errors in the estimate of energy values are within  $1000\text{ cm}^{-1}$  except for the transitions at  $25000\text{ cm}^{-1}$  of Ser-137 ( $3000\text{ cm}^{-1}$ ), at  $38000\text{ cm}^{-1}$  of yeast SOD ( $3000\text{ cm}^{-1}$ ), at  $24600\text{ cm}^{-1}$  of Gln-132 ( $7000\text{ cm}^{-1}$ ), and at  $5900\text{ cm}^{-1}$  of Gln-132 Gln-133 ( $6000\text{ cm}^{-1}$ ); <sup>b</sup>values are taken from reference 9.

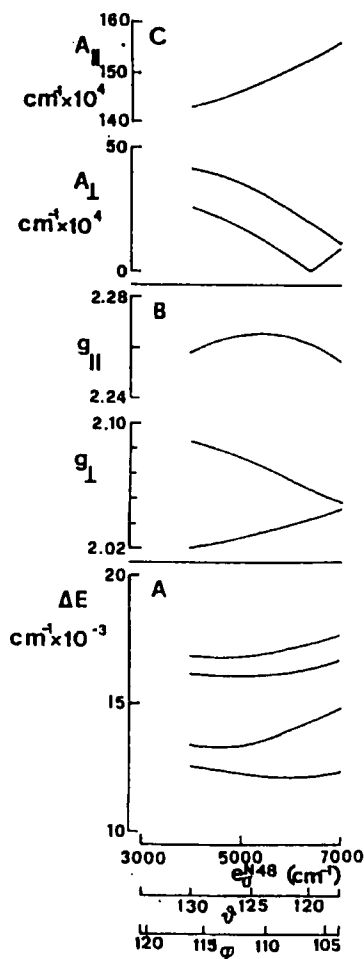


FIGURE 7 The effect of decreasing  $\theta$  and  $\rho$  of His-48 and simultaneously equalizing the  $e_{\sigma}$  values of the four histidines keeping their average  $e_{\sigma}/e_{\pi}$  ratio constant A) on the energy levels; B) on the  $g$  values; C) on the  $A$  values.

powerful way of deciphering the relationship between structure and function in SOD. The Nuclear Magnetic Resonance studies here have shown that as the 137-residue is changed, the water that is present at the active site in the wild type enzyme is gradually eliminated. Concomitant with that, CD studies have shown a geometric change around the active site from a more tetrahedral to a more square planar structure.

Activity studies (pulse radiolysis) have shown that rather than the presence or absence of  $\text{H}_2\text{O}$ , or the tetrahedral versus square planar coordination geometry of copper(II), the charge on the residues near the active site cavity plays the primary role in determining the catalytic efficiency of the enzyme.

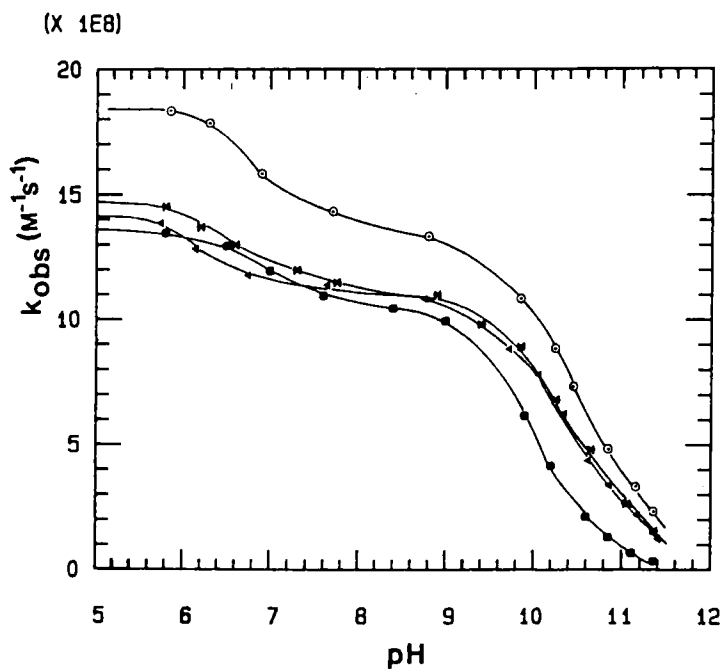


FIGURE 8 pH dependence of specific activity of wild type SOD ( $\circ$ ), Ser-137 ( $*$ ), Ala-137 ( $\blacktriangle$ ), Ile-137 ( $\bullet$ ). The solid lines simply connect the experimental values.

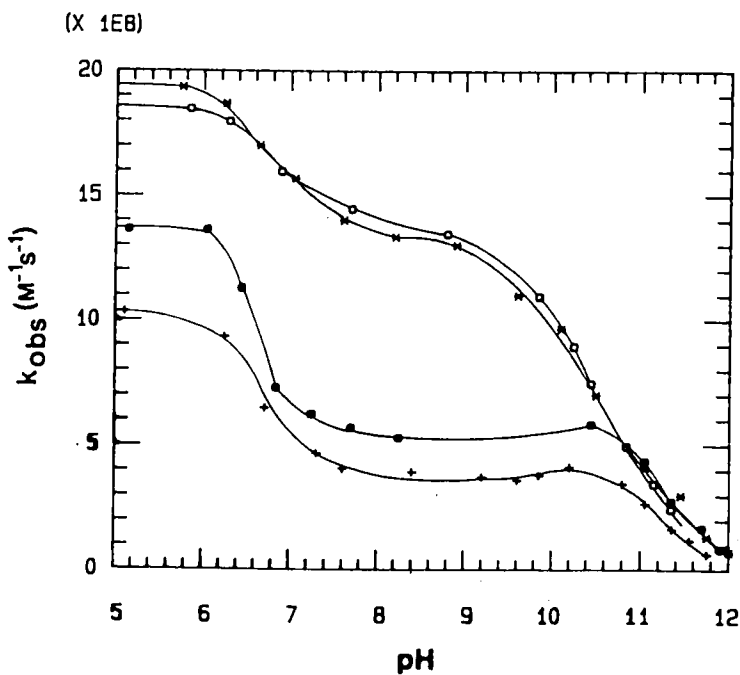


FIGURE 9 pH dependence of specific activity of wild type SOD ( $\circ$ ), Gln-132 ( $*$ ), Gln-133 ( $+$ ), Gln-132Gln-133 ( $\bullet$ ). The solid lines simply connect the experimental values.

## References

1. J.A. Fee (1981) in *Metal Ions in Biological Systems*, (ed. H. Sigel), Marcel Dekker, New York, vol. 13, pp. 259–298.
2. J.S. Valentine and M.W. Pantoliano (1981) in *Copper Proteins*, (ed. T.G. Spiro), Wiley, New York, vol. 3, pp. 291–358.
3. L. Banci, I. Bertini, C. Luchinat and M. Piccioli (1990) *Coordination Chemistry Reviews*, **100**, 67.
4. J.A. Tainer, E.D. Getzoff, K.M. Beem, J.S. Richardson and D.C. Richardson (1982) *Journal of Molecular Biology*, **160**, 181–217.
5. J.A. Tainer, E.D. Getzoff, J.S. Richardson and D.C. Richardson (1983) *Nature*, **306**, 284–287.
6. H.M. Steinman, V.R. Naik, J.L. Abernethy and R.L. Hill (1974) *Journal of Biological Chemistry*, **249**, 7326–7338.
7. J.R. Jabusch, D.L. Farb, D.A. Kerschensteiner and H.F. Deutsch (1980) *Biochemistry*, **19**, 2310–2316.
8. J.T. Johansen, C. Verballe-Petersen, B. Martin, V. Hasemann and I. Svendsen (1979) *Carlsberg Research Communications*, **44**, 201–217.
9. M.W. Pantoliano, J.S. Valentine and L.A. Nafie (1982) *Journal of the American Chemical Society*, **104**, 6310–6317.
10. K. Krogh-Jespersen and H.J. Schugar (1984) *Inorganic Chemistry*, **L23**, 4390–4393.
11. a) R.G. Brigg and J.A. Fee (1978) *Biochimica et Biophysica Acta*, **537**, 86–89; b) R.A. Liebermann, R.H. Sands and J.A. Fee (1982) *Journal of Biological Chemistry*, **257**, 336–344; c) L. Banci, I. Bertini, R.A. Hallewell, C. Luchinat, and M.S. Viezzoli (1989) *European Journal of Biochemistry*, **184**, 125–129.
12. P. Gaber, R. Brown III, S.H. Koenig and J.A. Fee (1972) *Biochimica et Biophysica Acta*, **271**, 1–15.
13. I. Bertini, F. Briganti, C. Luchinat, M. Mancini and G. Spina (1985) *Journal of Magnetic Resonance*, **63**, 41–55.
14. I. Bertini and C. Luchinat (1986) *NMR of Paramagnetic Molecules in Biological Systems*, Benjamin/Cummings, Menlo Park, CA.
15. I. Bertini, L. Banci and C. Luchinat (1988) in *American Chemical Society Series: Metal Clusters in Proteins* (ed. L. Que, Jr.), vol. 372, pp. 70–84.
16. I. Bertini, G. Lanini, C. Luchinat, L. Messori, R. Monnanni and A. Scozzafava (1985) *Journal of the American Chemical Society*, **107**, 4391–4396.
17. L. Banci, I. Bertini, C. Luchinat and A. Scozzafava (1987) *Journal of the American Chemical Society*, **109**, 2328–2334.
18. L. Banci, I. Bertini, C. Luchinat, M. Piccioli, A. Scozzafava and P. Turano (1989) *Inorganic Chemistry*, **28**, 4650.
19. C.E. Schäffer (1968) *Structure and Bonding*, **5**, 68–95.
20. S.E. Harnung and C.E. Schäffer (1972) *Structure and Bonding*, **12**, 201–255.
21. A. Bencini (1982) *Coordination Chemistry Reviews*, **60**, 131–161.
22. L. Banci, A. Bencini, I. Bertini, C. Luchinat and M.S. Viezzoli, *Gazzetta Chimica Italiana*, in press.
23. I. Bertini, L. Banci, C. Luchinat and R.A. Hallewell (1988) in *Annals of the New York Academy of Sciences* (eds. H.W. Blanch and A.M. Klivanov), **542**, 37–52.
24. R.A. Hallewell, R. Mills, P. Tekamp-Olson, R. Blacher, S. Rosenberg, F. Otting, F.R. Masiarz and C.J. Scandella (1987) *Biotechnology*, **5**, 363–367.
25. R.A. Hallewell, F.R. Masiarz, R.C. Najarian, J.P. Puma, M.R. Quiroga, A. Randolph, R. Zanchez-Pescador, C.J. Scandella, B. Smith, K.S. Steimer and G.T. Mullenbach (1985), *Nucleic Acids Research*, **13**, 2017–2026.
26. L. Banci, I. Bertini, D. Cabelli, R.A. Hallewell, C. Luchinat, M.S. Viezzoli, *Inorg. Chem.*, in press.
27. I. Bertini, L. Banci, C. Luchinat, B.H.J. Bielski, D.E. Cabelli, G.T. Mullenbach and R.A. Hallewell (1989) *Journal of the American Chemical Society*, **111**, 714–719.
28. W.F. Beyer, I. Fridovich, G.T. Mullenbach and R.A. Hallewell (1987) *Journal of Biological Chemistry*, **262**, 11182–11287.
29. L. Banci, I. Bertini, C. Luchinat, and R.A. Hallewell (1988) *Journal of the American Chemical Society*, **110**, 3629–3633.
30. I. Bertini, C. Luchinat and L. Messori (1987) *Metal Ions in Biological Systems* (ed. H. Sigel), Marcel Dekker, New York, vol. 21, pp. 47–87.
31. I. Bertini, F. Briganti and C. Luchinat (1986) *Advanced Magnetic Resonance Techniques in Systems of High Molecular Complexity* (eds. N. Nicolai and G. Valensin), Birkhäuser, pp. 165–195.
32. J.S. Valentine, M.W. Pantoliano, P.J. McDonnell, A.R. Burger, S.J. Lippard (1979) *Proceedings of the National Academy of Sciences, USA*, **76**, 4245–4249.

33. D.E. Cabelli and B.H.J. Bielski (1983) *Journal of Physical Chemistry*, **87**, 1809-1812.
34. W.F. Beyer, I. Fridovich, G.T. Mullenbach and R.A. Hallewell (1987) *Journal of Biological Chemistry*, **23**, 11182-11187.
35. R.A. Hallewell, D. Cabelli and B.H.J. Bielski, unpublished results.

Accepted by Prof. G. Czapski